The bone and cartilage interplay in osteoarthritis: key to effective treatment strategy

Tuerlings, M.

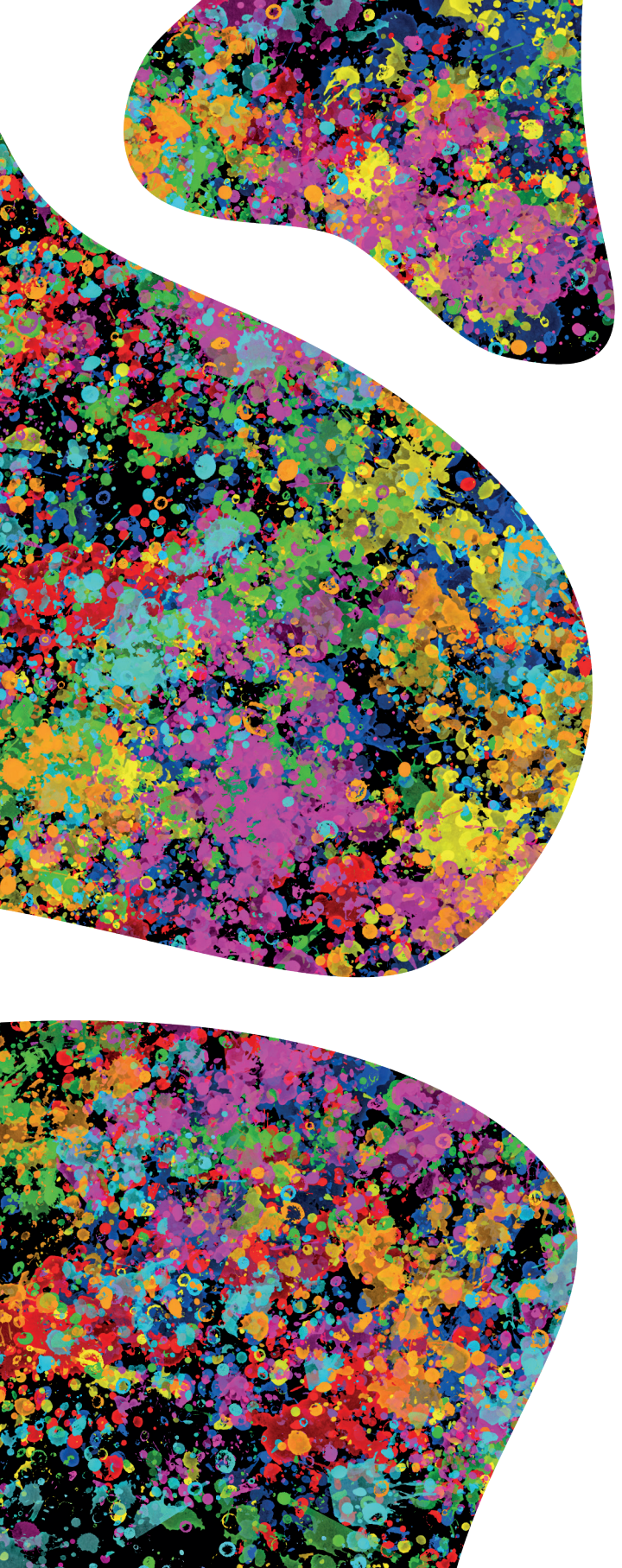

CHAPTER 6

WWP2 confers risk to osteoarthritis by affecting cartilage matrix deposition via hypoxia associated genes

Margo Tuerlings[1], George M.C. Janssen[2], Ilja Boone[1], Marcella van Hoolwerff[1], Alejandro Rodriguez Ruiz[1], Evelyn Houtman[1], H. Eka D. Suchiman[1], Robert J.P. van der Wal [3], Rob G.H.H. Nelissen[3], Rodrigo Coutinho de Almeida[1], Peter A. van Veelen[2], Yolande F.M. Ramos[1], Ingrid Meulenbelt[1]

[1] Dept. of Biomedical Data Sciences, Leiden University Medical Center, Leiden, The Netherlands.
[2] Center for proteomics and metabolomics , Leiden University Medical Center, Leiden, The Netherlands
[3] Dept. Orthopaedics Leiden University Medical Center, Leiden, The Netherlands.

Osteoarthritis and Cartilage, volume 31, issue 1 , January 2023, pages 39-48
DOI: 10.1016/j.joca.2022.09.009

Abstract

Objective: To explore the co-expression network of the osteoarthritis (OA) risk gene *WWP2* in articular cartilage and study cartilage characteristics when mimicking the effect of OA risk allele rs1052429-A on *WWP2* expression in a human 3D *in vitro* model of cartilage.

Method: Co-expression behavior of *WWP2* with genes expressed in lesioned OA articular cartilage (N=35 samples) was explored. By applying lentiviral particle mediated *WWP2* upregulation in 3D *in vitro* pellet cultures of human primary chondrocytes (N=8 donors) the effects of upregulation on cartilage matrix deposition was evaluated. Finally, we transfected primary chondrocytes with miR-140 mimics to evaluate whether miR-140 and WWP2 are involved in similar pathways.

Results: Upon performing Spearman correlations in lesioned OA cartilage, 98 highly correlating genes ($|\rho|>0.7$) were identified. Among these genes, we identified *GJA1*, *GDF10*, *STC2*, *WDR1*, and *WNK4.* Subsequent upregulation of WWP2 on 3D chondrocyte pellet cultures resulted in a decreased expression of *COL2A1* and *ACAN* and an increase in *EPAS1* expression. Additionally, we observed a decreased expression of *GDF10, STC2,* and *GJA1*. Proteomics analysis identified 42 proteins being differentially expressed with WWP2 upregulation, which were enriched for ubiquitin conjugating enzyme activity. Finally, upregulation of miR-140 in 2D chondrocytes resulted in significant upregulation of *WWP2* and *WDR1*.

Conclusion: Mimicking the effect of OA risk allele rs1052429-A on *WWP2* expression initiates detrimental processes in the cartilage shown by a response in hypoxia associated genes *EPAS1,GDF10,* and *GJA1* and a decrease in anabolic markers, *COL2A1* and *ACAN*.

Introduction

Globally, osteoarthritis (OA) is a highly prevalent and disabling joint disease which confers high social and economic burden to society. Risk factors for OA include sex, abnormal joint loading, obesity, metabolic diseases, and genetic factors [1]. To discover genes and underlying disease pathways, large genome wide association meta-analyses have been performed and multiple robust single nucleotide polymorphisms (SNPs) were identified significantly conferring risk to initiation and progression of OA [2-4]. Similar to other complex traits, these risk alleles have subsequently been found to affect expression of positional genes *in cis* in disease relevant tissues, also known as allelic imbalance (AI)[5 ,6]. Founded by this mechanism, we previously used RNA sequencing data of OA articular cartilage to report on genome-wide AI expression of SNPs in cartilage specific genes, as such, providing an AI expression database to *in silico* check functional aspects of identified and/or future OA risk SNPs [7]. One of the top findings was SNP rs1052429 located in the 3'UTR of the *WWP2* gene showing highly significant AI, with risk allele rs1052429-A marking higher expression of *WWP2* relative to rs1052429-G. Among the OA risk SNPs identified in a large genome-wide meta-analysis of Icelandic and UK knee OA patients was rs34195470, located in *WWP2* gene and a proxy of our AI SNP rs1052429 (r^2=0.6) [2]. Recently, rs34195470 was confirmed being OA risk SNP in the largest genome-wide meta-analysis so far, including individuals from 9 populations [4]. Based on these data, we could make a firm hypothesis that *WWP2,* with risk alleles rs34195470-G and rs1052429-A, confers robust risk to human OA which is marked by increased expression of *WWP2*. We also previously identified transcription of *WWP2* in cartilage being epigenetically regulated [8], as well as being responsive in the OA pathophysiological process [9]. Moreover, *WWP2* was previously shown to be a marker for hypertrophic chondrocytes in OA knee joints [10].

WWP2 is a member of the Nedd4 superfamily, a small group within the E3 ubiquitin ligase enzymes and is involved in post-translational modifications. The WWP2 protein contains four double tryptophan (WW) domains, which allow specific protein-protein interactions and it is expressed in multiple organs throughout the body [11]. More specifically to cartilage, Nakamura et al. [12] showed that WWP2 interacts with SOX9 to form a complex that facilitates nuclear translocation of SOX9, as such enabling SOX9 transcriptional activity. Despite the association between the risk allele and higher expression levels of *WWP2* in human cartilage, the effect of *WWP2* knockout (KO) in mice with age-related and surgically induced models of OA showed that lack of *WWP2* expression resulted in increased expression of catabolic cartilage markers *RUNX2* and *ADAMTS5* [13]. In a different context, *WWP2* was found to be a host gene for microRNA-140 (miR-140), a miRNA highly expressed in cartilage and shown to be differentially expressed between preserved and lesioned OA cartilage [9]. As such, it

was suggested that expression of miR-140 and the C-terminal transcript of *WWP2* (*WWP2-C*, also called *WWP2* isoform 2) are co-regulated [14 ,15].

In the current study, we set out to explore how increased levels of *WWP2*, conferring risk to OA, affect cartilage matrix. To get gain insight in the *WWP2* pathway, we started with exploring a *WWP2* co-expression network in our previous whole-transcriptome OA cartilage dataset [9]. Moreover, to study the effect of the genetic risk allele (increased levels of *WWP2*), we functionally assessed the effect of lentiviral-mediated upregulation of *WWP2* in a 3D *in vitro* model using primary human chondrocytes. Apart from conventional anabolic and catabolic cartilage markers, genes identified in the *WWP2* co-expression network were used as a read-out to evaluate the effect of *WWP2* upregulation. Since WWP2 is involved in post-translational modifications, we explored the effect of *WWP2* upregulation on protein level by performing proteomic analysis. Finally, we explored the effects of upregulation of miR-140 in primary chondrocytes by transfection with miR-140 mimics.

Methods

Sample description

All material included in this study is obtained as part of the Research Arthritis and Articular Cartilage (RAAK) study. The RAAK-study is aimed at biobanking of joint materials of patients who underwent a total joint replacement surgery due to OA. Classification of macroscopically preserved and lesioned OA cartilage was done as described previously [16]. For all sample characteristics see **Supplementary Table 1**. The RAAK-study is approved by the medical ethics committee of the Leiden University Medical Center (P08.239/P19.013).

RNA-sequencing

Lesioned OA cartilage was collected from hip and knee joints (N=35 samples), snap frozen in liquid nitrogen, pulverized and homogenized in TRIzol (Invitrogen), and RNA was isolated using Qiagen RNeasy Mini Kit (Qiagen). Paired-end 2×100 bp RNA-sequencing (Illumina HiSeq2000 and Illumina HiSeq4000) was performed. Data from both Illumina platforms were integrated and analyzed with the same in-house pipeline. Additional details are described in **Supplementary methods.**

Creating a co-expression network

We explored co-expression behavior of WWP2 with progression of OA by correlating (Spearman correlation) *WWP2* expression levels in our RNA sequencing dataset with expression levels of all genes expressed in OA articular cartilage (N=20048 genes) [9]. To correct for multiple testing, the Benjamini-Hochberg method was used, as

indicated by the false discovery rate (FDR), with a significance cutoff value of 0.05. To include the most informative genes a threshold of $|\rho|>0.7$ and FDR<0.05 were selected, corresponding to approximately the top 1% of the total significant correlations.

Lentiviral transduction
The full length WWP2 plasmid was digested and inserted into the XhoI/XbaI sites of the pLV-CMV-IRES-eGFP lentiviral backbone (kindly provided by Prof. Dr. Hoeben). The pLV-CMV-IRES-eGFP lentiviral backbone without the WWP2 insert was used as a control. Additional details are available in the **Supplementary methods**.

In vitro 3D pellet cultures
3D pellet cultures were formed by adding 2.5x105 cells in their expansion medium to a 15 ml Falcon tube and subsequently expose them to centrifugal forces (1200 rpm, 4 minutes). Chondrogenesis was initiated in serum-free chondrogenic differentiation medium. Additional details are available in the **Supplementary methods**.

RT-qPCR
RNA was isolated from the samples using the RNeasy Mini Kit (Qiagen). cDNA synthesis was performed using the First Strand cDNA Synthesis Kit (Roche Applied Science). Subsequently, RT-qPCR was performed adjusting for housekeeping genes GAPDH and SDHA. Additional details are available in the **Supplementary methods**.

Quantitative Proteomics Using TMT Labeling
Lysis, digestion, TMT labeling and mass spectrometry analysis was essentially performed as described previously [8]. All searches and subsequent data analysis, including Percolator and abundance ratio calculation, were performed using Proteome Discoverer 2.4 (Thermo Scientific). Additional details are available in the **Supplementary methods**.

Histochemistry
Sections of the 3D chondrocyte pellet culutes were stained for glycosaminoglycan (GAG) deposition using the Alcian Blue staining. The staining was quantified using Fiji. Additional details are available in **Supplementary methods**.

Transfection with miR-140 mimics
Primary chondrocytes were transfected with hsa-miR-3p mimic (Invitrogen) or a control mimic at 5 nM final concentration using Opti-MEM (Gibco) and Lipofectamine RNAiMax Transfection reagent (Invitrogen) according to manufacturer's protocol. Additional details are available in **Supplementary methods.**

An overview of the applied strategy can be seen in **Figure 1**. The RNA sequencing data of the articular cartilage is deposited at ArrayExpress (E-MTAB-7313). Further data generated and used in this study is not openly available due to reasons of sensitivity and are available from the corresponding author upon reasonable request.

Results

Co-expression network of WWP2

To identify genes that are regulated by, or co-expressed with, *WWP2* in OA cartilage, we used RNA sequencing data of lesioned OA cartilage (N=35 samples, **Supplementary Table 1A**) to perform Spearman correlation between expression levels of *WWP2* and genes expressed in cartilage (N=20048 genes, **Supplementary Table 2, Figure 1A**). We identified 98 genes highly correlating ($|\rho|>0.7$) to *WWP2*. These 98 genes were significantly enriched for, amongst others, GO-terms Extracellular exosome (GO:0070062, 36 genes), characterized by expression of *GJA1* (encoding gap junction alpha 1), *SMO* (encoding smoothened frizzled class receptor), and *WDR1* (encoding WD repeat domain 1), and Myelin sheath (GO:0043209, 10 genes), characterized by expression of *WDR1, RALA* (encoding RAS like proto-oncogene A), and *CCT5* (encoding chaperonin containing TCP1 subunit 5) (**Supplementary Table 3**). As shown in **Supplementary Figure 1**, genes highly correlating to *WWP2* (N=98) formed a highly interconnected network, i.e. genes that are all highly correlating with each other. In this network we identified direct and indirect relations with *WWP2*, including *GJA1* (ρ=-0.81, 70 connections, i.e. highly correlating to 70 genes in the network), *WNK4* (encoding WNK lysine deficient protein kinase 4, ρ=0.81, 37 connections), *ACAN* (encoding aggrecan, ρ=0.78, 16 connections), and *STC2* (encoding stanniocalcin 2, ρ=0.77, 17 connections).

Lentiviral particle-mediated upregulation of WWP2

The effect of upregulation of *WWP2* was studied on cartilaginous matrix deposition in *in vitro* 3D chondrocyte pellet cultures, by creating a lentiviral particle mediated upregulation of *WWP2*. 3D pellet cultures were harvested after three or seven days of culturing and gene (N=16 pellet cultures of N=8 donors) and protein (N=16 pellet cultures of N=4 donors) expression levels were measured (**Supplementary Table 1B**). First, we confirmed whether *WWP2* upregulation was successful by measuring both gene and protein expression levels at day zero of the 3D chondrocyte pellet culture, and we observed a significant increase in *WWP2* gene expression levels ($P=1.0x10^{-5}$, **Supplementary Figure 2A and supplementary Figure 2B**), which was confirmed on protein level ($P=3.2x10^{-6}$, **Supplementary Figure 2C**).

Effect of WWP2 upregulation on cartilage matrix deposition

Next, we evaluated effect of *WWP2* upregulation on expression levels of conventional

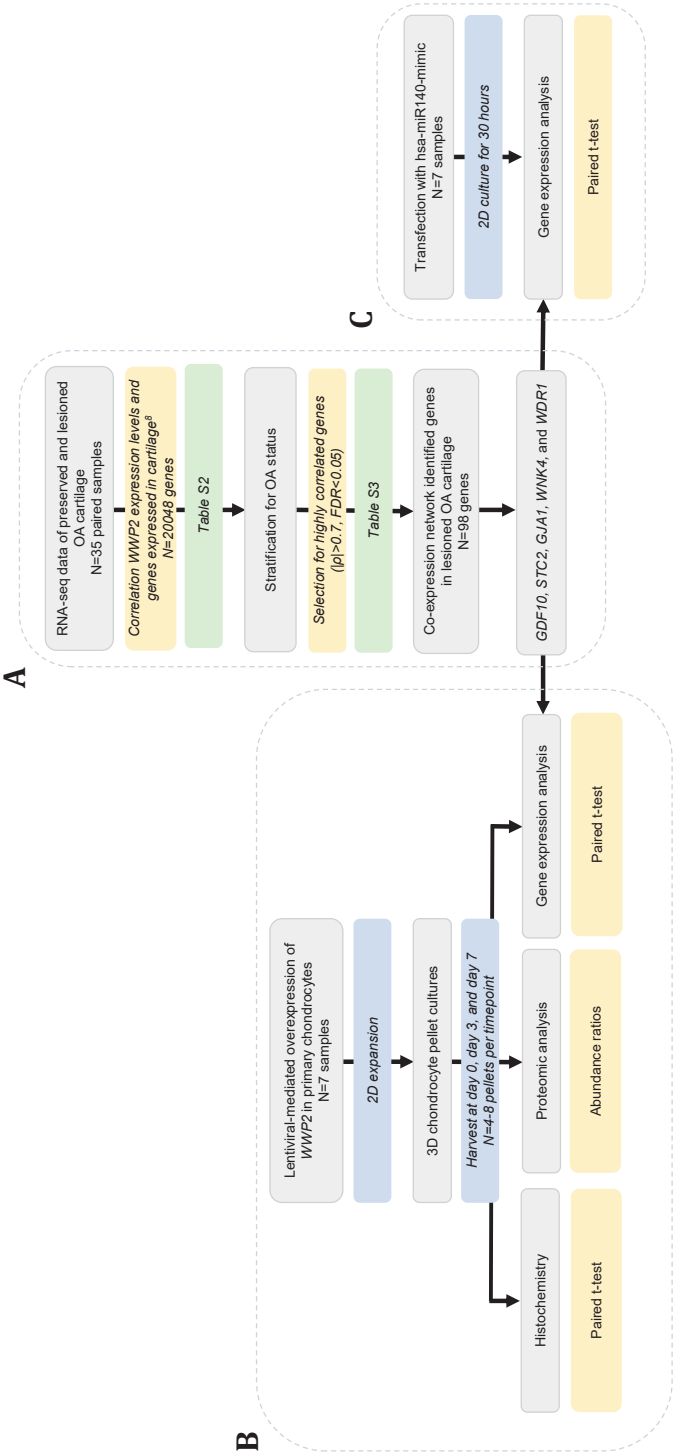

Figure 1 – Schematic overview of applied strategy.

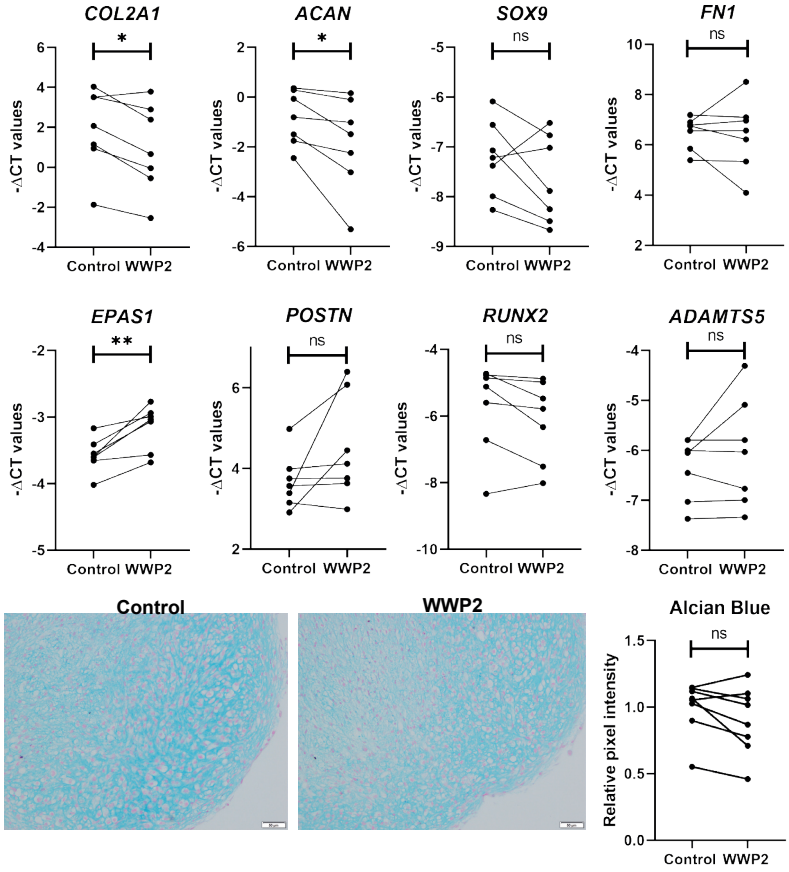

Figure 2 – mRNA expression levels of cartilage matrix markers (A) and cartilage degeneration markers (B) for pellets with WWP2 upregulation and their controls at day 7 (N=11-12 pellet cultures, N=7 donors). (C) Alcian Blue staining visualizing GAGs deposition in WWP2 overexpressed pellets and their controls after 7 days of culturing (N= 26 pellet cultures, N=8 donors).
The scale bar indicates 50 um. Ns: not significant. *P<0.05, ** P<0.005 upon performing a Paired sample t-test.

cartilage genes during 3D pellet culture of seven days (**Figure 1B**). As shown in **Figure 2A**, we found significant reduced gene expression of *ACAN* (FC=0.80, *P*=0.04) and *COL2A1* (encoding collagen type 2 alpha chain 1, FC=0.77, *P*=0.01), in *WWP2* upregulated pellets compared to their controls at day seven (**Supplementary Table 4**). Moreover, we showed significant increased gene expression of degeneration markers *EPAS1* (encoding endothelial PAS domain protein 1, FC=1.56, *P*=0.004) (**Figure 2B**). Notably, *SOX9*, *ADAMTS5,* and *RUNX2*, which were previously linked to WWP2 function, were not consistently changed upon WWP2 upregulation. Moreover, we stained 3D pellet cultures for presence of glycosaminoglycans (GAGs) using Alcian Blue staining, and observed a trend towards decreased Alcian Blue intensity when comparing *WWP2*

upregulated pellets with controls (**Figure 2C**).

Effect of WWP2 upregulation on genes correlated to WWP2

To investigate functional relationships between *WWP2* and identified correlating and highly interconnected genes, we selected *GDF10* (encoding growth differentiation factor 10, ρ=0.72, 18 connections), *STC2* (ρ=0.77, 17 connections), *GJA1* (ρ=-0.81, 70 connections), *WDR1* (encoding WD repeat-containing protein 1, ρ=-0.70, 5 connections), and *WNK4 (*ρ=0.81, 37 connections) from the network (**Supplementary Figure 1**) to use as read-out of WWP2 upregulation in 3D chondrocyte pellet cultures (**Figure 1B**). As shown in **Figure 3**, we observed significant decreased gene expression of *GDF10* (FC=0.62, *P*=0.002) and *STC2* (FC=0.73, *P*=0.04) with upregulation of *WWP2*. Albeit not significant, gene expression of *GJA1* (FC=0.76, *P*=0.08) was also consistently lower in *WWP2* upregulated pellets. Together, these data suggest that *GDF10*, *STC2*, and *GJA1* are downstream of *WWP2* either by direct or indirect activity. In contrast, *WNK4* and *WDR1* did not show consistent changes in expression with upregulation of *WWP2*, suggesting *WNK4* and *WDR1* are rather upstream in the pathway of *WWP2.*

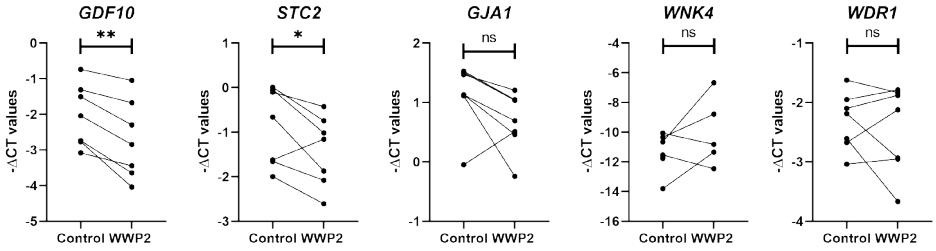

Figure 3 – mRNA expression levels of genes correlating with WWP2 in WWP2 upregulated 3D chondrocyte pellet cultures compared to their controls after 7 days of culturing (N=6-12 pellet cultures, N=7 donors).
Ns: not significant, * P<0.05, ** P<0.05 upon performing a Paired sample t-test.

Proteomics

To study the extent to which gene expression levels translate to protein levels, we performed proteomics analysis. Prior to differential expression analysis of pellet cultures with and without WWP2 upregulation, we explored protein expression levels of cartilage markers in our control pellet cultures at day three and day seven of 3D pellet culture. Upon comparing day three and day seven with day zero of control pellets, we observed increased protein expression of cartilage markers COL2A1 (FC=2.68 and FC=32.94, respectively), ACAN (FC=5.28 and FC=13.75, respectively), COMP (cartilage oligomeric matrix protein, FC=5.31 and FC=20.25, respectively), and FN1 (fibronectin, FC=2.12 and FC=3.51, respectively) (**Supplementary Table 5, Supplementary Figure**

3). Moreover, mesenchymal markers CD44 (FC=0.83 and FC=0.46, respectively) and CD166 (FC=0.79 and FC=0.62, respectively) and IGFBP3 (insulin growth factor binding protein 3, FC=0.10 and FC=0.10, respectively) were downregulated on both days. Together, this indicates that cartilage-like matrix is produced by chondrocytes already at day three, but is increasing towards day seven. Notably, SOX9 was not detected in the proteomics analysis.

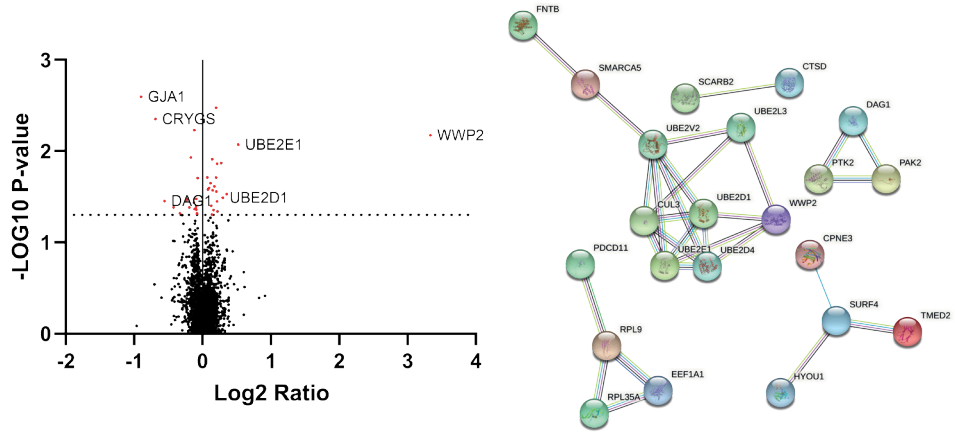

Figure 4 – Results of proteomics comparing WWP2 transduced 3D pellet cultures and their controls. (A) Volcano plot of proteins differentially expressed between WWP2 transduced 3D pellet cultures and their controls at day three and day seven together (N=16 pellets, N=4 donors). The red dots indicate the significantly differentially expressed proteins. (B) Protein-protein interaction network in STRING.

Next, we evaluated the effect of WWP2 upregulation on cartilage matrix deposition on protein level (**Figure 1B**). Since we observed increased protein expression of cartilage markers in control pellet cultures already on day three (**Supplementary Figure 3A**), we pooled day three and day seven for further analysis to increase power. Upon comparing pellet cultures with and without WWP2 upregulation, we found WWP2 still being significantly upregulated after three and seven days of culturing. Furthermore, we found 42 proteins significantly differentially expressed (**Figure 4A, Supplementary Table 6**), of which GJA1 (FC=0.54) was most significantly downregulated in WWP2 upregulated pellet cultures, confirming the downregulation observed on gene expression level (FC=0.76). Oppositely, the observed changes in *ACAN, COL2A1, FN1,* and *POSTN* gene expression levels were not confirmed on protein level. Proteins encoded by *SOX9, EPAS1, RUNX2,* and *ADAMTS5* were either not identified or did not show unique peptides. Upon performing enrichment analysis on the 42 differentially expressed proteins, we found significant enrichment for ubiquitin conjugating enzyme activity (5 proteins, FDR=0.002) and ubiquitin-protein transferase activity (6 proteins, FDR=0.03), both terms characterized by expression of, amongst others, UBE2D4, UBE2L3, and UBE2D1. Furthermore, these 42 proteins showed significant protein-protein interactions

(P=0.02, **Figure 4B**), also representing ubiquitin conjugating enzyme activity.

miR-140-3p and WWP2

Since it has been suggested that *WWP2* and miR-140 are co-expressed [14 ,15], we transfected primary chondrocytes with miR-140-3p mimics, to assess whether this miRNA regulates *WWP2* expression or similar genes as involved in the *WWP2* co-expression network (N=7, **Supplementary Table 1B**, **Figure 1C**). To investigate whether miR-140-3p regulates *WWP2,* we first evaluated the effects of miR-140-3p mimic on expression levels of *WWP2* full length and *WWP2* splice variants isoform 2, isoform 4, and isoform 6 (**Supplementary Figure 4**). MiR-140 is suggested to be co-

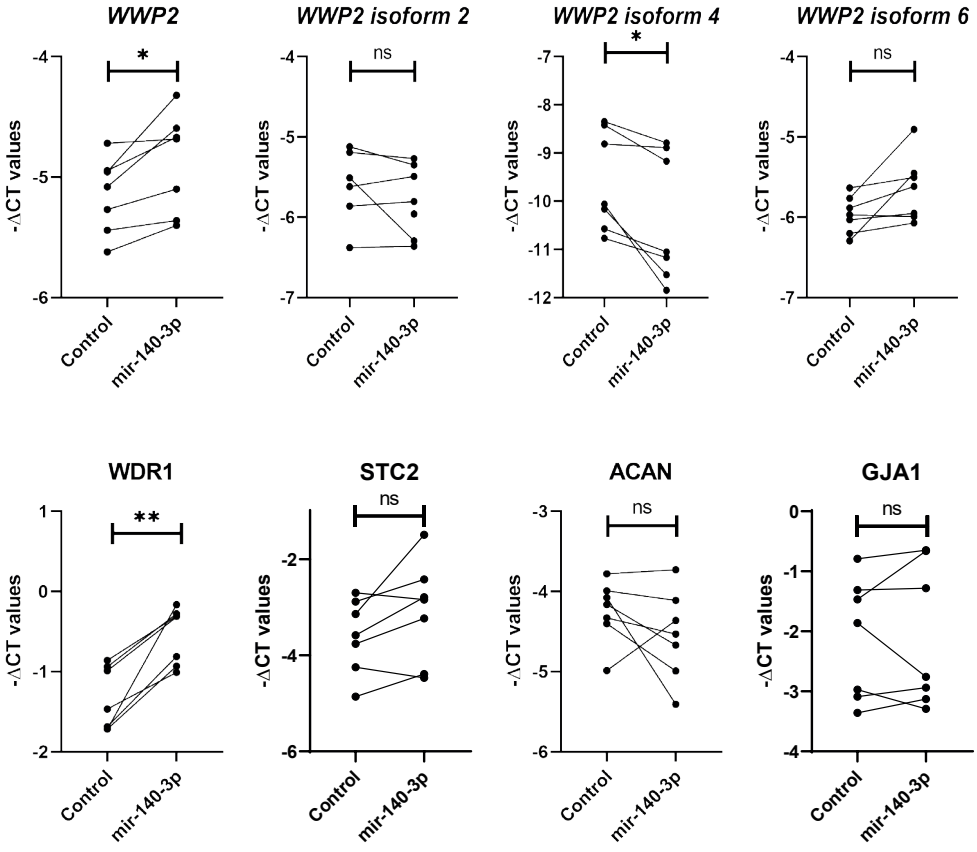

Figure 5 – mRNA expression levels upon transfection with miR-140-3p.
(A) expression levels of WWP2 and its isoforms. (B) Expression levels of genes correlated to WWP2 (N=8 wells, N=4 donors). Ns: not significant, * p<0.05, ** p<0.005 upon performing a Paired sample t-test.

expressed with splice variant *WWP2* isoform 2, also called *WWP2-C,* as they share the promotor [15]. Isoform 4 is also known as *WWP2-N* and is a transcript that does not contain miR-140 (**Supplementary Figure 4**). As shown in **Figure 5A**, we observed significant increased expression levels of *WWP2* (FC=1.22, *P*=0.02) with upregulation of miR-140-3p. Moreover, we observed consistent increased expression of *WWP2* isoform 6 (FC=1.29, *P*=0.06), while significant decreased expression of isoform 4 (FC=0.63, *P*=0.02) (**Supplementary Table 7**). Notably, we did not see effect on expression levels of *WWP2* isoform 2, also called *WWP2-C*. With respect to highly correlated genes, we observed increased expression of *WDR1* (FC=1.79, $P=1.00x10^{-3}$), one of the genes that was not consistently changed with *WWP2* upregulation (**Figure 5B**). Albeit not significant, we observed an increased expression of *STC2* (FC=1.55, *P*=0.08), which is also contradictory to the effects of *WWP2* upregulation. Moreover, we did not observe consistent effects on *GJA1* expression levels.

Discussion

By combining a genome-wide screen for cartilage specific allelic imbalance [7] and large scale GWAS [2 ,4], we hypothesized that upregulated expression of *WWP2* confers robust risk to OA. Here, we set out to functionally investigate the role of *WWP2* in cartilage by exploring the *WWP2* co-expression network in a previously assessed RNA sequencing dataset [9]. Moreover, lentiviral-mediated upregulation of *WWP2* was shown to have detrimental effects on cartilage matrix deposition, as shown by downregulation of *COL2A1* and *ACAN* and upregulation of *EPAS1*. Apart from conventional anabolic and catabolic cartilage markers, genes identified in the *WWP2* co-expression network were used as read-out, showing *GDF10*, *STC2*, and *GJA1* being responsive to *WWP2* upregulation. Furthermore, to explore effects of miR-140-3p, that was suggested to be co-regulated with *WWP2,* we transfected primary chondrocytes with miR-140-3p mimics.

Based on AI expression of the OA risk SNP rs1052429, we hypothesized that *WWP2* confers risk to OA onset by upregulated expression, whereas *WWP2* exhibited FDR significantly lower expression in lesioned compared to preserved cartilage (FC=0.78, $FDR=5.3x10^{-3}$), together suggesting that lower expression levels of *WWP2* in lesioned OA cartilage are rather an attempt of chondrocytes to reverse the OA state than a cause to the OA process [23 ,24]. Concomitantly, co-expression network analyses showed 98 highly and significantly ($|\rho|>0.7$, FDR<0.05) correlating genes to *WWP2*, including *GJA1* ($\rho=-0.81$), *WNK4* ($\rho=0.81$), *ACAN* ($\rho=0.78$), and *STC2* ($\rho=0.77$) (**Supplementary Table 2**). Previously, it was shown that WWP2 interacts with SOX9 and that it regulates SOX9 transcriptional activity [12]. Although *SOX9* is highly expressed in cartilage, *SOX9* was not among the high and significant correlations ($\rho=0.5$). On the other hand, *SOX9* was

previously shown to regulate the expression of, amongst others *ACAN* [25 ,26], which was here shown to be highly correlated to *WWP2* (ρ=0.78).

Upon studying the effect of upregulation of *WWP2*, we found *EPAS1* and *GDF10* being genes that had most consistent and significant changed levels of gene expression. *EPAS1*, encoding hypoxia-inducible factor 2 alpha, is known for its role in endochondral ossification and is a known cartilage degradation marker in OA [27 ,28]. *GDF10*, also known as bone morphogenic protein 3, is involved in osteogenesis as it inhibits osteoblast differentiation via *SMAD2* and *SMAD3 [24 ,29]*. The latter also being previously identified as OA susceptibility gene [2]. Furthermore, lower expression level of *GDF10* was associated with OA severity in both bone and cartilage [30]. Interestingly, *GDF10* was shown to be a hypoxia inducible gene, like *EPAS1*, which is regulated by SOX9 and was identified as marker for differentiated chondrocytes as it inhibits adipogenesis and osteogenesis [31]. Both *EPAS1* and *GDF10* were not in the proteomics analysis, either because they were not measured (EPAS1) or they did not show unique peptides (GDF10). Additionally, we observed a decrease in *STC2* and *GJA1* expression. Downregulation of *GJA1* did not reach statistical significance on gene expression level, while on protein level GJA1 was the most significantly downregulated protein. STC2 is a glycoprotein and upregulation of *STC2* in mice has been shown to delay endochondral ossification [32 ,33]. Moreover, it was shown that *STC2* was higher expressed in healthy cartilage compared to osteophytic cartilage [34], suggesting its potential role in initiation and progression of OA in presence of higher *WWP2* expression. GJA1, also known as connexin 43, is a major protein of functional gap junctions which allows for cell-cell communication. More specific to cartilage, connexin 43 is essential in mechanotransduction [35]. Alterations in connexin 43 expression and localization affects this cell-cell communication, by which homeostasis to maintain cartilage tissue gets disturbed [36]. Notably, like EPAS1 and GDF10, the function of connexin 43 is regulated by oxygen levels [37]. Upregulation of *EPAS1* and downregulation of *GDF10*, *STC2* and *GJA1* suggests that increased level of WWP2 has detrimental effects on cartilage matrix deposition, which acts via hypoxia associated chondrocyte dedifferentiation. This is in line with decreased gene expression levels of *COL2A1* and *ACAN,* two major cartilage markers.

To evaluate the effects of WWP2 upregulation on cartilage matrix deposition on protein level, we performed proteomics analysis. We did confirm upregulation of WWP2 on day zero, which was still present at day three and seven (**Figure 4, Supplementary Figure 2,**). Moreover, we found 42 significantly differentially expressed proteins upon comparing pellet cultures with and without WWP2 upregulation, of which GJA1 was most significantly differentially expressed and showing the highest fold change (FC=0.49). We were not able to confirm differences we observed in gene expression

levels of *COL2A1*,*ACAN*,*FN1,* and *POSTN* on protein level (**Supplementary Table 6**), which might be due to the relatively low sample size (N=4 donors) or due to suboptimal timepoint chosen to evaluate the effect of WWP2 on either gene or protein expression level. Since WWP2 is a E3 ubiquitin ligase and the differentially expressed proteins were significantly enriched for ubiquitin conjugating enzyme activity and ubiquitin-protein transferase activity, upregulation of WWP2 could also affect proteins cellular location, activity, and protein-protein interactions without changing expression levels itself, which is not captured by our read-outs. Moreover, it should be noted that the here observed fold differences were relatively low and additional validation and replication are necessary.

Since it has been suggested that miR-140 is co-expressed with *WWP2-C* [14], *WWP2* isoform 2, we generated upregulation of miR-140 in 2D primary chondrocytes to explore whether *WWP2* and miR-140 are involved in similar pathways. In the miR-140 upregulated cells, we observed significant increased expression levels of *WWP2,* indicating miR-140 indeed targets *WWP2*. Nonetheless, given the predicted *WWP2* target site of miR-140 (3'UTR of *WWP2* isoform 6 [38]) and the absence of SNPs in this region in linkage disequilibrium with the OA risk SNP rs1052429, the genetic *WWP2* risk nor the allelic imbalance is brought about via an aberrant miR-140 binding to *WWP2*. The fact that we did not observe consistent changes in expression levels of *WWP2* isoform 2, suggests that *WWP2* isoform 2 and miR-140 indeed share the intron 10 (*WWP2* full length) promotor as hypothesized previously by Rice at al. [15]. Additional research is required to fully understand the role of miR-140 in the *WWP2* pathway and in OA pathophysiology in general.

Although lower expression of *WWP2* was observed in lesioned compared to preserved cartilage in our previous study [9], genetic evidence suggests that higher expression of *WWP2* predisposes to development of OA, indicating that downregulation in OA pathophysiology is merely a response to the pathophysiological process and a beneficial attempt of chondrocytes to reverse the OA state [7]. The latter shows that genes identified being differentially expressed between preserved and lesioned OA articular cartilage are a response to the OA pathophysiological process and not necessarily causal to the OA pathophysiological process. To identify genes causal to OA, genetic studies have to be performed. To our surprise, Styrkarsdottir et al. [2] reported on *WWP2* expression in adipose tissue as function of SNP rs4985453-G, a proxy of their identified OA risk allele rs34195470-G (R^2=0.79) and our AI SNP rs1052429-A (R^2=0.77), highlighting the OA risk allele being associated with lower expression levels of *WWP2*. Upon investigating the GTEx eQTL data of *WWP2* with the highlighted SNPs [39], we found only data showing consistently higher expression of *WWP2* as function of OA risk alleles of the

respective SNPs across multiple tissues (**Supplementary Figure 5**), underscoring the aberrant effects observed here with *WWP2* upregulation. Although Mokuda et al. [13] showed that lack of *WWP2* expression in mice resulted in increased expression of *RUNX2* and *ADAMTS5*, we here did not observe consistent changes in expression of *RUNX2* or *ADAMTS5* upon upregulation of *WWP2* in our human chondrocyte pellet cultures and culturing for seven days. This difference could be due to translational limitations from mice to humans. Alternatively, we here create neocartilage, and the effect on *RUNX2* and *ADAMTS5* may be a temporal or time-dependent effect, which we do not observe at day seven of culturing.

In conclusion, our data provide support to our hypothesis that high levels of *WWP2* have detrimental effects on cartilage homeostasis. We identified *EPAS1, GJA1, GDF10,* and *STC2*, all genes involved in chondrocyte dedifferentiation, to be involved in the *WWP2* pathway. Moreover, we showed that miR-140 is likely involved in similar pathways as *WWP2* and miR-140 might play a role in regulating *WWP2* expression. Together these data contribute to a better understanding of how *WWP2* confers risk to OA and is a step towards translation from bench to bedside.

Declarations

Acknowledgements

We thank all the participants of the RAAK study. The LUMC has and is supporting the RAAK study. We thank all the members of our group for valuable discussion and feedback. We also thank Enrike van der Linden, Demiën Broekhuis, Peter van Schie, Shaho Hasan, Maartje Meijer, Daisy Latijnhouwers, Anika Rabelink-Hoogenstraaten, and Geert Spierenburg for collecting the RAAK material. We thank the Sequence Analysis Support Core (SASC) of the Leiden University Medical Center for their support. The study was funded by the Dutch Scientific Research council NWO/ZonMW VICI scheme (nr 91816631/528), Dutch Arthritis Society (DAA_10_1-402), BBMRI-NL complementation project (CP2013-83), European Commission Seventh Framework programme (TreatOA, 200800), and Ana fonds (O2015-27). Data is generated within the scope of the Medical Delta programs Regenerative Medicine 4D: Generating complex tissues with stem cells and printing technology and Improving Mobility with Technology.

Funding

The study was funded by the Dutch Scientific Research council NWO /ZonMW VICI scheme (nr 91816631/528), Dutch Arthritis Society (DAA_10_1-402), BBMRI-NL complementation project (CP2013-83), European Commission Seventh Framework programme (TreatOA, 200800), and Ana fonds (O2015-27).

Disclosures

The authors have no relevant financial or non-financial interests to disclose.

References

1. Vina ER, Kwoh CK. Epidemiology of osteoarthritis: literature update. *Curr Opin Rheumatol* 2018;30(2):160-67. doi: 10.1097/bor.0000000000000479 [published Online First: 2017/12/12]
2. Styrkarsdottir U, Lund SH, Thorleifsson G, Zink F, Stefansson OA, Sigurdsson JK, et al. Meta-analysis of Icelandic and UK data sets identifies missense variants in SMO, IL11, COL11A1 and 13 more new loci associated with osteoarthritis. *Nat Genet* 2018;50(12):1681-87. doi: 10.1038/s41588-018-0247-0 [published Online First: 2018/10/31]
3. Zengini E, Hatzikotoulas K, Tachmazidou I, Steinberg J, Hartwig FP, Southam L, et al. Genome-wide analyses using UK Biobank data provide insights into the genetic architecture of osteoarthritis. *Nat Genet* 2018;50(4):549-58. doi: 10.1038/s41588-018-0079-y [published Online First: 2018/03/22]
4. Boer CG, Hatzikotoulas K, Southam L, Stefánsdóttir L, Zhang Y, Coutinho de Almeida R, et al. Deciphering osteoarthritis genetics across 826,690 individuals from 9 populations. *Cell* 2021 doi: 10.1016/j.cell.2021.07.038 [published Online First: 2021/08/28]
5. Gee F, Clubbs CF, Raine EV, Reynard LN, Loughlin J. Allelic expression analysis of the osteoarthritis susceptibility locus that maps to chromosome 3p21 reveals cis-acting eQTLs at GNL3 and SPCS1. *BMC Med Genet* 2014;15:53. doi: 10.1186/1471-2350-15-53 [published Online First: 2014/06/03]
6. Raine EV, Dodd AW, Reynard LN, Loughlin J. Allelic expression analysis of the osteoarthritis susceptibility gene COL11A1 in human joint tissues. *BMC Musculoskelet Disord* 2013;14:85. doi: 10.1186/1471-2474-14-85 [published Online First: 2013/03/19]
7. den Hollander W, Pulyakhina I, Boer C, Bomer N, van der Breggen R, Arindrarto W, et al. Annotating Transcriptional Effects of Genetic Variants in Disease-Relevant Tissue: Transcriptome-Wide Allelic Imbalance in Osteoarthritic Cartilage. *Arthritis Rheumatol* 2019;71(4):561-70. doi: 10.1002/art.40748 [published Online First: 2018/10/10]
8. den Hollander W, Ramos YF, Bomer N, Elzinga S, van der Breggen R, Lakenberg N, et al. Transcriptional associations of osteoarthritis-mediated loss of epigenetic control in articular cartilage. *Arthritis Rheumatol* 2015;67(8):2108-16. doi: 10.1002/art.39162 [published Online First: 2015/04/22]
9. Coutinho de Almeida R, Ramos YFM, Mahfouz A, den Hollander W, Lakenberg N, Houtman E, et al. RNA sequencing data integration reveals an miRNA interactome of osteoarthritis cartilage. *Annals of the rheumatic diseases* 2019;78(2):270-77. doi: 10.1136/annrheumdis-2018-213882 [published Online First: 2018/12/07]
10. Ji Q, Zheng Y, Zhang G, Hu Y, Fan X, Hou Y, et al. Single-cell RNA-seq analysis reveals the progression of human osteoarthritis. 2019;78(1):100-10. doi: 10.1136/annrheumdis-2017-212863 %J Annals of the Rheumatic Diseases
11. Chantry A. WWP2 ubiquitin ligase and its isoforms: new biological insight and promising disease targets. *Cell Cycle* 2011;10(15):2437-9. doi: 10.4161/cc.10.15.16874 [published Online First: 2011/07/14]
12. Nakamura Y, Yamamoto K, He X, Otsuki B, Kim Y, Murao H, et al. Wwp2 is essential for palatogenesis mediated by the interaction between Sox9 and mediator subunit 25. *Nat Commun* 2011;2:251. doi: 10.1038/ncomms1242 [published Online First: 2011/03/24]
13. Mokuda S, Nakamichi R, Matsuzaki T, Ito Y, Sato T, Miyata K, et al. Wwp2 maintains cartilage homeostasis through regulation of Adamts5. *Nature Communications* 2019;10(1):2429. doi: 10.1038/s41467-019-10177-1
14. Yang J, Qin S, Yi C, Ma G, Zhu H, Zhou W, et al. MiR-140 is co-expressed with Wwp2-C transcript and activated by Sox9 to target Sp1 in maintaining the chondrocyte proliferation. *FEBS Lett* 2011;585(19):2992-7. doi: 10.1016/j.febslet.2011.08.013 [published Online First: 2011/08/30]
15. Rice SJ, Beier F, Young DA, Loughlin J. Interplay between genetics and epigenetics in osteoarthritis. *Nature Reviews Rheumatology* 2020;16(5):268-81. doi: 10.1038/s41584-020-0407-3
16. Ramos YF, den Hollander W, Bovee JV, Bomer N, van der Breggen R, Lakenberg N, et al. Genes involved in the osteoarthritis process identified through genome wide expression analysis in articular cartilage; the RAAK study. *PloS one* 2014;9(7):e103056. doi: 10.1371/journal.pone.0103056 [published Online First: 2014/07/24]
17. Wu TD, Watanabe CK. GMAP: a genomic mapping and alignment program for mRNA and EST sequences. *Bioinformatics* 2005;21(9):1859-75. doi: 10.1093/bioinformatics/bti310 [published Online First: 2005/02/25]
18. Anders S, Pyl PT, Huber W. HTSeq--a Python framework to work with high-throughput sequencing data. *Bioinformatics* 2015;31(2):166-9. doi: 10.1093/bioinformatics/btu638 [published Online First: 2014/09/28]
19. Ewels P, Magnusson M, Lundin S, Kaller M. MultiQC: summarize analysis results for multiple tools and samples in a single report. *Bioinformatics* 2016;32(19):3047-8. doi: 10.1093/bioinformatics/btw354 [published Online First: 2016/06/18]
20. Love MI, Huber W, Anders S. Moderated estimation of fold change and dispersion for RNA-seq data with DESeq2. *Genome Biology* 2014;15(12):550. doi: 10.1186/s13059-014-0550-8
21. Bomer N, den Hollander W, Ramos YF, Bos SD, van der Breggen R, Lakenberg N, et al. Underlying molecular mechanisms of DIO2 susceptibility in symptomatic osteoarthritis. *Annals of the rheumatic diseases* 2015;74(8):1571-9. doi: 10.1136/annrheumdis-2013-204739 [published Online First: 2014/04/04]
22. Pirro M, Mohammed Y, van Vliet SJ, Rombouts Y, Sciacca A, de Ru AH, et al. N-Glycoproteins Have a Major Role in MGL Binding to Colorectal Cancer Cell Lines: Associations with Overall Proteome Diversity. *Int J Mol Sci* 2020;21(15) doi: 10.3390/ijms21155522 [published Online First: 2020/08/06]
23. Reynard LN. Analysis of genetics and DNA methylation in osteoarthritis: What have we learnt about the disease? *Semin Cell Dev Biol* 2017;62:57-66. doi: 10.1016/j.semcdb.2016.04.017 [published Online First: 2016/05/01]
24. Rice SJ, Cheung K, Reynard LN, Loughlin J. Discovery and analysis of methylation quantitative trait loci (mQTLs) mapping to novel osteoarthritis genetic risk signals. *Osteoarthritis Cartilage* 2019;27(10):1545-56. doi: 10.1016/j.joca.2019.05.017 [published Online First: 2019/06/08]
25. Sekiya I, Tsuji K, Koopman P, Watanabe H, Yamada Y, Shinomiya K, et al. SOX9 enhances aggrecan gene promoter/enhancer activity and is up-regulated by retinoic acid in a cartilage-derived cell line, TC6. *J Biol Chem* 2000;275(15):10738-44. doi: 10.1074/jbc.275.15.10738 [published Online First: 2001/02/07]
26. Nishimura R, Hata K, Takahata Y, Murakami T, Nakamura E, Yagi H. Regulation of Cartilage Development and Diseases by Transcription Factors. *J Bone Metab* 2017;24(3):147-53. doi: 10.11005/jbm.2017.24.3.147 [published Online First: 2017/09/29]
27. Yang S, Kim J, Ryu JH, Oh H, Chun CH, Kim BJ, et al. Hypoxia-inducible factor-2alpha is a catabolic regulator of osteoarthritic cartilage destruction. *Nat Med* 2010;16(6):687-93. doi: 10.1038/nm.2153 [published Online First: 2010/05/25]

28. Saito T, Fukai A, Mabuchi A, Ikeda T, Yano F, Ohba S, et al. Transcriptional regulation of endochondral ossification by HIF-2alpha during skeletal growth and osteoarthritis development. *Nat Med* 2010;16(6):678-86. doi: 10.1038/nm.2146 [published Online First: 2010/05/25]
29. Matsumoto Y, Otsuka F, Hino J, Miyoshi T, Takano M, Miyazato M, et al. Bone morphogenetic protein-3b (BMP-3b) inhibits osteoblast differentiation via Smad2/3 pathway by counteracting Smad1/5/8 signaling. *Mol Cell Endocrinol* 2012;350(1):78-86. doi: 10.1016/j.mce.2011.11.023 [published Online First: 2011/12/14]
30. Chou CH, Lee CH, Lu LS, Song IW, Chuang HP, Kuo SY, et al. Direct assessment of articular cartilage and underlying subchondral bone reveals a progressive gene expression change in human osteoarthritic knees. *Osteoarthritis Cartilage* 2013;21(3):450-61. doi: 10.1016/j.joca.2012.11.016 [published Online First: 2012/12/12]
31. Lafont JE, Talma S, Hopfgarten C, Murphy CL. Hypoxia promotes the differentiated human articular chondrocyte phenotype through SOX9-dependent and -independent pathways. *J Biol Chem* 2008;283(8):4778-86. doi: 10.1074/jbc.M707729200 [published Online First: 2007/12/14]
32. Gagliardi AD, Kuo EY, Raulic S, Wagner GF, DiMattia GE. Human stanniocalcin-2 exhibits potent growth-suppressive properties in transgenic mice independently of growth hormone and IGFs. *Am J Physiol Endocrinol Metab* 2005;288(1):E92-105. doi: 10.1152/ajpendo.00268.2004 [published Online First: 2004/09/16]
33. Chang AC, Hook J, Lemckert FA, McDonald MM, Nguyen MA, Hardeman EC, et al. The murine stanniocalcin 2 gene is a negative regulator of postnatal growth. *Endocrinology* 2008;149(5):2403-10. doi: 10.1210/en.2007-1219 [published Online First: 2008/02/09]
34. Gelse K, Ekici AB, Cipa F, Swoboda B, Carl HD, Olk A, et al. Molecular differentiation between osteophytic and articular cartilage--clues for a transient and permanent chondrocyte phenotype. *Osteoarthritis Cartilage* 2012;20(2):162-71. doi: 10.1016/j.joca.2011.12.004 [published Online First: 2012/01/03]
35. Gago-Fuentes R, Bechberger JF, Varela-Eirin M, Varela-Vazquez A, Acea B, Fonseca E, et al. The C-terminal domain of connexin43 modulates cartilage structure via chondrocyte phenotypic changes. *Oncotarget* 2016;7(45):73055-67. doi: 10.18632/oncotarget.12197 [published Online First: 2016/09/30]
36. Mayan MD, Gago-Fuentes R, Carpintero-Fernandez P, Fernandez-Puente P, Filgueira-Fernandez P, Goyanes N, et al. Articular chondrocyte network mediated by gap junctions: role in metabolic cartilage homeostasis. *Annals of the rheumatic diseases* 2015;74(1):275-84. doi: 10.1136/annrheumdis-2013-204244 [published Online First: 2013/11/15]
37. Knight MM, McGlashan SR, Garcia M, Jensen CG, Poole CA. Articular chondrocytes express connexin 43 hemichannels and P2 receptors - a putative mechanoreceptor complex involving the primary cilium? *J Anat* 2009;214(2):275-83. doi: 10.1111/j.1469-7580.2008.01021.x [published Online First: 2009/02/12]
38. Agarwal V, Bell GW, Nam J-W, Bartel DP. Predicting effective microRNA target sites in mammalian mRNAs. *eLife* 2015;4:e05005. doi: 10.7554/eLife.05005
39. The Genotype-Tissue Expression (GTEx) project. *Nat Genet* 2013;45(6):580-5. doi: 10.1038/ng.2653 [published Online First: 2013/05/30]

Supplementary files

Supplementary methods

RNA-sequencing

Lesioned OA cartilage was collected from macroscopically lesioned areas (based on color of the articular cartilage, surface integrity, and depth of the cartilage upon sampling with scalpel) of hip and knee joints and snap frozen in liquid nitrogen. Subsequently, the cartilage was pulverized and homogenized in TRIzol reagent (Invitrogen) using mixer mill 200 (Retsch). RNA was isolated from the articular cartilage using Qiagen RNeasy Mini Kit (Qiagen, GmbH, Hilden, Germany). Paired-end 2×100 bp RNA-sequencing (Illumina TruSeq RNA Library Prep Kit, Illumina HiSeq2000 and Illumina HiSeq4000) was performed. Strand specific RNA-seq libraries were generated which yielded a mean of 20 million reads per sample. Data from both Illumina platforms were integrated and analyzed with the same in-house pipeline. RNA-seq reads were aligned using GSNAP [2] against GRCh38 using default parameters. Read abundances per sample was estimated using HTSeq count v0.11.1 [3]. Only uniquely mapping reads were used for estimating expression. The quality of the raw reads for RNA-sequencing was checked using MultiQC v1.7. [4]. To identify outliers, principal component analysis (PCA) was applied. The DESeq2 package [5] was used to normalize the RNA-seq data, as a variance-stabilizing transformation was performed.

Lentiviral transduction

The full length WWP2 plasmid (NM_001270454.1) was ordered in pcDNA3.1 with XhoI/XbaI cloning sites (Genscript Biotech). The plasmid was digested and inserted into the XhoI/XbaI sites of the pLV-CMV-IRES-eGFP lentiviral backbone (kindly provided by Prof. Dr. Hoeben, Dept. of Molecular Cell Biology, Leiden University Medical Center). Lentiviral production was performed in HEK 293T cells, using Lenti-vpak Lentiviral Packaging Kit (Origene Technologies, Inc.). The HEK 293T cells were expanded in DMEM (high glucose; Gibco) supplemented with 10% fetal calf serum (FBS, Gibco) and 100 U/ml penicillin and 100 ug/ml streptomycin (Gibco). The pLV-CMV-IRES-eGFP lentiviral backbone without the WWP2 insert was used as a control. Primary chondrocytes were isolated from the articular cartilage of human joints and expanded in DMEM (high glucose; Gibco) supplemented with 10% FBS (Gibco), 100 U/ml penicillin and 100 ug/ml streptomycin (Gibco), and 0.5 ng/ml FGF-2 (PeproTech), as described previously [7]. After expansion, the chondrocytes were seeded in a density of 3.5x105 cells per 10 cm culture dish (passage 2) and left overnight. Then, the lentivirus was added in a MOI of 1 in addition of 15 ug/ml Polybrene (Sigma-Aldrich). After incubation of approximately 16 hours, the lentiviral solution was replaced by normal culture medium. The chondrocytes were passaged and expanded afterwards.

In vitro 3D pellet cultures

Primary chondrocytes were isolated from macroscopically preserved cartilage of OA hip and knee joints by incubating the cartilage overnight in expansion medium (DMEM (high glucose; Gibco), supplemented with 10% fetal bovine serum (FBS; Gibco), 100 U/ml penicillin and 100 ug/ml streptomycin (Gibco), 0.5 ng/ml FGF-2 (PeproTech)) in addition of 2 mg/ml collagenase type I. To remove undigested cartilage fragments, the primary chondrocytes were then resuspended, filtered through a 100 µm mesh and plated in a culture dish with expansion medium. 3D pellet cultures were formed by adding 2.5x105 cells in their expansion medium to a 15 ml Falcon tube and subsequently expose them to centrifugal forces (1200 rpm, 4 minutes). After 24 hours, the expansion medium was replaced by chondrogenic differentiation medium (DMEM (high glucose; Gibco), supplemented with Ascorbic acid (50 µg/ml; Sigma-Aldrich), L-Proline (40 µg/ml; Sigma-Aldrich), Sodium Puryvate (100 µg/ml; Sigma-Aldrich), Dexamethasone (0.1 µM; Sigma-Aldrich), ITS+, 100 U/ml penicillin and 100 ug/ml streptomycin (Gibco) and TGF-β1 (10 ng/ml; PeproTech)), as described previously [7]. Medium was refreshed every 3-4 days and the caps of the Falcon tubes were open for the first 7 days to allow oxygen entering the tubes. The pellets were harvested at different timepoints; after 24 hours (day 0) and after 7 days. The harvested materials were lysed using RNABee (Bio-connect) and stored at -80oC until further processing.

RT-qPCR

RNA was isolated from the samples using the RNeasy Mini Kit (Qiagen). cDNA synthesis was performed using the First Strand cDNA Synthesis Kit (Roche Applied Science). Subsequently, RT-qPCR was performed with the Biomark™ 96.96 Dynamic Arrays (Fluidigm) according to the manufacturer's protocol. Additional RT-qPCR was performed using SYBR Green without the ROX reference dye (Roche Applied Science) and the QuantStudio 6 Real-Time PCR system (Applied Biosystems). In both methods, GAPDH and SDHA were used as housekeeping genes. The measured gene expression levels were corrected for the housekeeping genes GAPDH and SDHA, and the fold changes were calculated using the 2-ΔΔCT method. All values were calculated relative to the control groups. The paired sample t-test was used to calculate significance ($P<0.05$).

Quantitative Proteomics Using TMT Labeling

Lysis, digestion, TMT labeling and mass spectrometry analysis was essentially performed as described [8]. In short, 3D pellet cultures were washed with PBS, extracted with 100 ul 5% SDS, 100 mM Tris HCl pH 7.6 each, sonicated twice for 10 min and incubated for 20 min at 95°C. Insoluble material was removed by centrifugation for 2 minutes at 15,000 rpm in an Eppendorf centrifuge. Proteins were reduced, alkylated, subjected to chloroform methanol precipitation and digested with trypsin as described earlier [8].

Peptide concentration was determined by BCA Gold protein assay (Pierce) and 10ug of the peptide was labeled using TMT10plex reagent (Thermo). Three separate TMT10 sets were prepared with a common reference sample consisting of a mixture of all peptide samples. TMT-labeled peptides were dissolved in 0.1% formic acid and subsequently analyzed by online C18 nano-HPLC MS/MS with a system consisting of an Easy nLC 1200 gradient HPLC system (Thermo, Bremen, Germany), and an Orbitrap Fusion LUMOS mass spectrometer in synchronous precursor selection (Thermo). For peptide identification, MS/MS spectra were searched against the human database (20596 entries) using Mascot Version 2.2.07 (Matrix Science) with the following settings: 10 ppm and 0.6 Da deviation for precursor and fragment masses, respectively. Trypsin was set as enzyme and two missed cleavages were allowed. Carbamidomethyl on cysteines and TMT6plex on Lys and N-term were set as fixed modifications. Variable modifications were oxidation (on Met and Pro) and acetylation on the protein N-terminus. All searches and subsequent data analysis, including Percolator and abundance ratio calculation, were performed using Proteome Discoverer 2.4 (Thermo Scientific). Peptide-spectrum matches were adjusted to a 1% FDR. Proteins were filtered on a minimal unique peptide count of 2. Since the sample size was rather small and we did observe significant increased expression of cartilage markers already at day three of pellet culture, we pooled the data of day 3 and day 7 for further analysis.

Histochemistry

The 3D chondrocyte pellet cultures were fixed with 4% formaldehyde and subsequently embedded in paraffin. The sections were stained for glycosaminoglycan (GAG) deposition using the Alcian Blue staining. The staining was quantified by loading the images in Fiji and splitting the color channels. Subsequently, the grey values were measured and corrected for the grey value of the background and for the number of cells present. The paired sample t-test was again used to calculate significance.

Transfection with miR-140 mimics

Primary chondrocytes were passaged in a concentration of 4.0x104 cells per well. After 24 hours, the cells were transfected with hsa-miR-140-3p mimic (Invitrogen) or a control mimic at 5 nM final concentration using Opti-MEM (Gibco) and Lipofectamine RNAiMax Transfection reagent (Invitrogen) according to manufacturer's protocol. These miRNA mimics are chemically modified double-stranded RNA molecules that mimic endogenous miRNAs, in this case miR-140-3p. The control mimic consists of a random miRNA sequence that does not have an effect in human tissues. Approximately 16 hours after transfection, the cells were lysed using TRizol (Thermo Fisher Scientific) for RNA isolation and stored at -80oC until further processing.

References

1. Rmos YF, den Hollander W, Bovee JV, Bomer N, van der Breggen R, Lakenberg N, et al. Genes involved in the osteoarthritis process identified through genome wide expression analysis in articular cartilage; the RAAK study. PloS one 2014;9(7):e103056. doi: 10.1371/journal.pone.0103056 [published Online First: 2014/07/24]
2. Wu TD, Watanabe CK. GMAP: a genomic mapping and alignment program for mRNA and EST sequences. Bioinformatics 2005;21(9):1859-75. doi: 10.1093/bioinformatics/bti310 [published Online First: 2005/02/25]
3. Anders S, Pyl PT, Huber W. HTSeq--a Python framework to work with high-throughput sequencing data. Bioinformatics 2015;31(2):166-9. doi: 10.1093/bioinformatics/btu638 [published Online First: 2014/09/28]
4. Ewels P, Magnusson M, Lundin S, Kaller M. MultiQC: summarize analysis results for multiple tools and samples in a single report. Bioinformatics 2016;32(19):3047-8. doi: 10.1093/bioinformatics/btw354 [published Online First: 2016/06/18]
5. Love MI, Huber W, Anders S. Moderated estimation of fold change and dispersion for RNA-seq data with DESeq2. Genome Biology 2014;15(12):550. doi: 10.1186/s13059-014-0550-8
6. Coutinho de Almeida R, Ramos YFM, Mahfouz A, den Hollander W, Lakenberg N, Houtman E, et al. RNA sequencing data integration reveals an miRNA interactome of osteoarthritis cartilage. Annals of the rheumatic diseases 2019;78(2):270-77. doi: 10.1136/annrheumdis-2018-213882 [published Online First: 2018/12/07]
7. Bomer N, den Hollander W, Ramos YF, Bos SD, van der Breggen R, Lakenberg N, et al. Underlying molecular mechanisms of DIO2 susceptibility in symptomatic osteoarthritis. Annals of the rheumatic diseases 2015;74(8):1571-9. doi: 10.1136/annrheumdis-2013-204739 [published Online First: 2014/04/04]
8. Pirro M, Mohammed Y, van Vliet SJ, Rombouts Y, Sciacca A, de Ru AH, et al. N-Glycoproteins Have a Major Role in MGL Binding to Colorectal Cancer Cell Lines: Associations with Overall Proteome Diversity. Int J Mol Sci 2020;21(15) doi: 10.3390/ijms21155522 [published Online First: 2020/08/06]

Supplementary figures

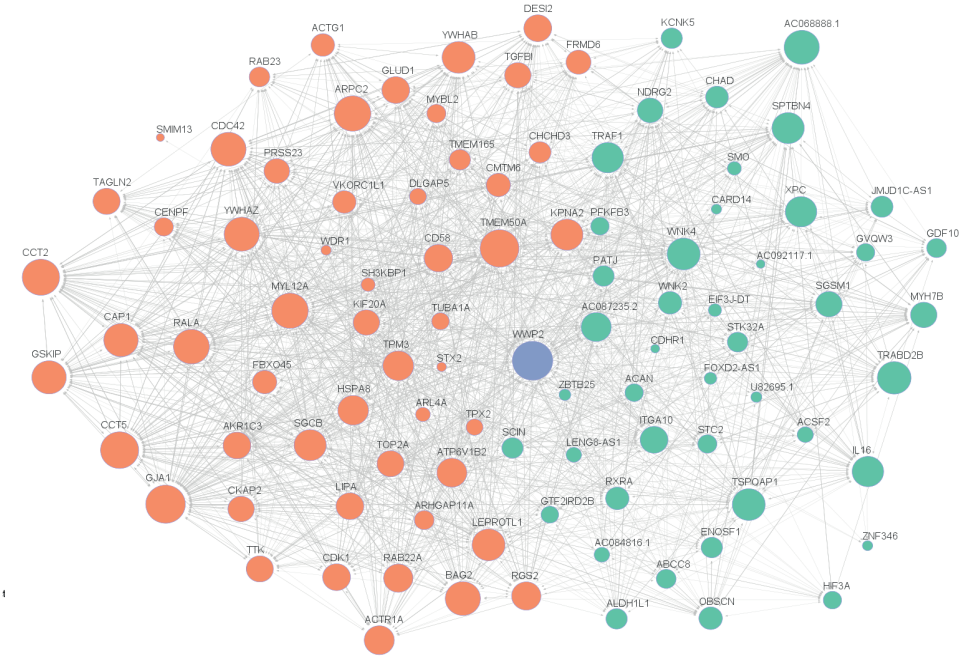

Supplementary Figure 1 - Interconnected network of genes highly correlating (|ρ|>0.7, FDR<0.05) to WWP2 in lesioned OA articular cartilage.
The positive correlations are shown in green and the negative correlations are shown in orange. The size of the nodes in the network indicate the number of connections.

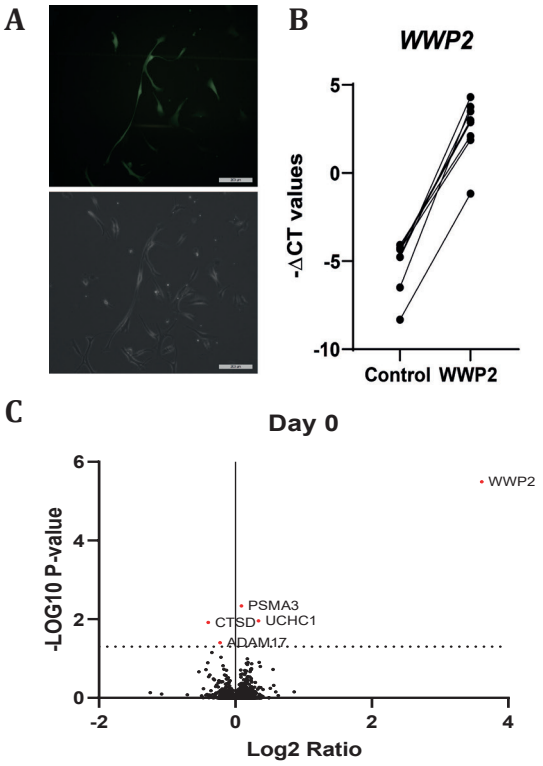

Supplementary Figure 2 – Overexpression of WWP2.
(A) Monolayer of chondrocytes 3 days after transduction. (B) -ΔCT values of WWP2 overexpressed pellets and their controls at day 0 of the 3D pellet culture. (C) Volcano plot of proteomics analysis at day 0 showing WWP2 being upregulated.

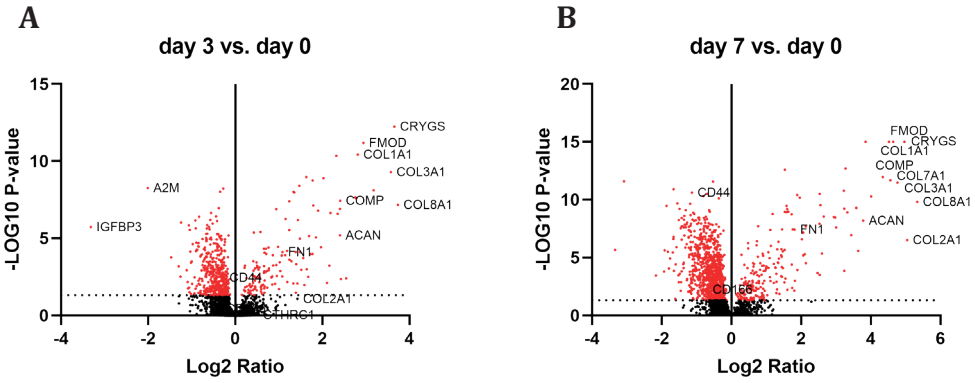

Supplementary Figure 3 – Volcano plot of proteins differentially expressed between day three and day zero (A) and day seven and day zero (B) of pellet culture in the control pellets (N=16 pellet cultures, N=4 donors)

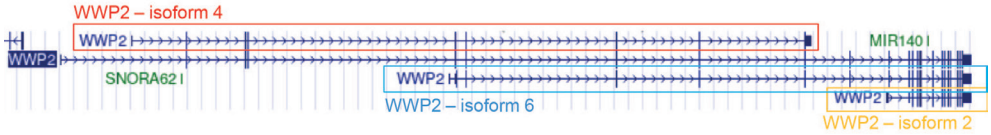

Supplementary Figure 4 – Overview of WWP2 transcripts as shown by UCSC genome browser.
WWP2 isoform 2, also called WWP2-C, is suggested to be co-expressed with miR-140, while WWP2 isoform 4, also called WWP2-N, does not contain miR-140.

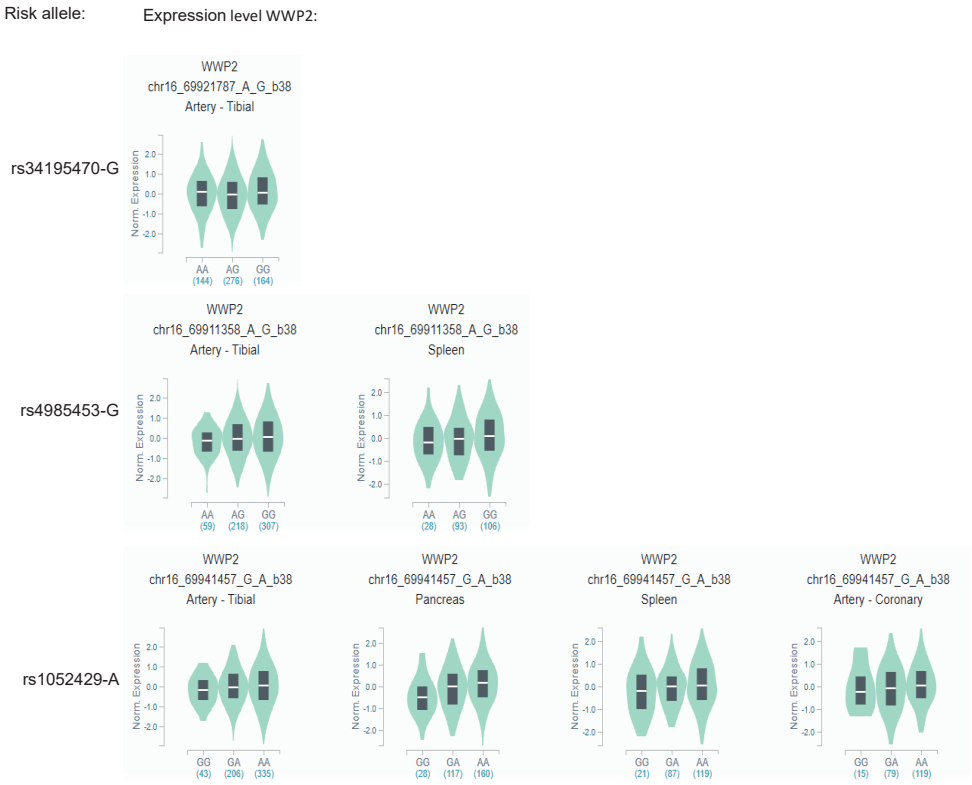

Supplementary Figure 5 – GTEx violin plots of WWP2 expression as function of the three OA susceptibility alleles.
In all three cases, the OA risk allele is associated to higher expression levels of WWP2 across multiple tissues.

Supplementary tables

Supplementary Table 1 – Baseline characteristics of material included in the current study
Supplementary Table 1A – Sample characteristics of RNA-seq data for correlation

	RNA-seq data (N=35)
Participants	35
Age (SD)	68,6 (9,0)
BMI (SD)*	28,3 (3,4)
Knees (Hips)	28 (7)
Females (Males)	27 (7)
*** Available for 21 out of 35 patients.**	

Supplementary Table 1B – Sample characteristics of functional experiments

	Lentiviral particle mediated overexpression of WWP2 (Gene expression, N=8)	**Lentiviral particle mediated overexpression of WWP2 (proteomics, N=4)**	**Transfection miR-140 (N=7)**
Age (SD)	71.1 (9.2)	75.5 (11.6)	71.6 (9.8)
Knees (Hips)	8 (0)	4 (0)	7 (0)
Females (Males)	5(3)	2 (2)	5(2)

Supplementary Table 2 (partially) - Spearman correlations between expression levels of WWP2 and genes expressed in articular cartilage (N=20048 genes) in lesioned OA cartilage samples.
The top 50 highest absolute correlations are shown here, the rest of the table can be found in the online supplement: https://doi.org/10.1016/j.joca.2022.09.009

Ensembl ID	Gene Name	ρ	P-value	FDR
ENSG00000256321	AC087235.2	0.84	3.26E-10	6.54E-06
ENSG00000152661	GJA1	-0.81	2.93E-09	2.93E-05
ENSG00000126562	WNK4	0.81	4.56E-09	3.04E-05
ENSG00000196715	VKORC1L1	-0.80	6.71E-09	3.36E-05
ENSG00000100744	GSKIP	-0.79	1.59E-08	5.64E-05
ENSG00000138107	ACTR1A	-0.79	1.75E-08	5.64E-05
ENSG00000269113	TRABD2B	0.79	1.97E-08	5.64E-05
ENSG00000112208	BAG2	-0.79	2.30E-08	5.76E-05
ENSG00000128602	SMO	0.78	2.89E-08	6.44E-05
ENSG00000112742	TTK	-0.78	4.36E-08	8.58E-05
ENSG00000182481	KPNA2	-0.77	4.95E-08	8.58E-05
ENSG00000089775	ZBTB25	0.77	5.13E-08	8.58E-05
ENSG00000113739	STC2	0.77	6.96E-08	1.01E-04
ENSG00000154767	XPC	0.77	7.08E-08	1.01E-04
ENSG00000150753	CCT5	-0.76	9.05E-08	1.19E-04
ENSG00000157766	ACAN	0.76	9.53E-08	1.19E-04
ENSG00000257337	AC068888.1	0.76	1.08E-07	1.22E-04
ENSG00000174013	FBXO45	-0.76	1.09E-07	1.22E-04
ENSG00000131747	TOP2A	-0.76	1.21E-07	1.24E-04
ENSG00000164626	KCNK5	0.76	1.30E-07	1.24E-04
ENSG00000256995	AC084816.1	0.76	1.30E-07	1.24E-04
ENSG00000141527	CARD14	0.76	1.36E-07	1.24E-04
ENSG00000111450	STX2	-0.75	1.66E-07	1.45E-04
ENSG00000131236	CAP1	-0.75	1.90E-07	1.52E-04
ENSG00000167037	SGSM1	0.75	1.90E-07	1.52E-04
ENSG00000147010	SH3KBP1	-0.75	2.13E-07	1.59E-04
ENSG00000158710	TAGLN2	-0.75	2.27E-07	1.59E-04
ENSG00000226696	LENG8-AS1	0.75	2.27E-07	1.59E-04
ENSG00000056558	TRAF1	0.75	2.31E-07	1.59E-04
ENSG00000166226	CCT2	-0.75	2.58E-07	1.70E-04
ENSG00000136457	CHAD	0.75	2.75E-07	1.70E-04
ENSG00000170312	CDK1	-0.75	2.75E-07	1.70E-04
ENSG00000183726	TMEM50A	-0.74	2.88E-07	1.70E-04

Ensembl ID	Gene Name	ρ	P-value	FDR
ENSG00000091317	CMTM6	-0.74	2.93E-07	1.70E-04
ENSG00000124209	RAB22A	-0.74	2.97E-07	1.70E-04
ENSG00000136108	CKAP2	-0.74	3.22E-07	1.72E-04
ENSG00000172349	IL16	0.74	3.22E-07	1.72E-04
ENSG00000150687	PRSS23	-0.74	3.27E-07	1.72E-04
ENSG00000148672	GLUD1	-0.74	3.59E-07	1.85E-04
ENSG00000184009	ACTG1	-0.74	3.76E-07	1.88E-04
ENSG00000186350	RXRA	0.74	3.88E-07	1.90E-04
ENSG00000132849	PATJ	0.74	4.06E-07	1.94E-04
ENSG00000276791	AC092117.1	0.74	4.45E-07	2.01E-04
ENSG00000104660	LEPROTL1	-0.74	4.52E-07	2.01E-04
ENSG00000116741	RGS2	-0.74	4.52E-07	2.01E-04
ENSG00000224963	U82695.1	0.74	4.66E-07	2.03E-04
ENSG00000144908	ALDH1L1	0.74	4.95E-07	2.07E-04
ENSG00000167552	TUBA1A	-0.74	4.95E-07	2.07E-04
ENSG00000006451	RALA	-0.73	5.50E-07	2.25E-04
ENSG00000163466	ARPC2	-0.73	6.48E-07	2.60E-04

Supplementary Table 3 - Significant gene enrichment of 98 genes correlating to WWP2

GO-term	Count	P-value	FDR	Genes
GO:0070062~extracellular exosome	36	1.94E-07	2.26E-05	RALA, SCIN, CDC42, WDR1, CMTM6, MYL12A, CHCHD3, LIPA, HSPA8, STX2, RAB23, CD58, TGFBI, RAB22A, SMO, CAP1, PATJ, ACTR1A, TPM3, ALDH1L1, ATP6V1B2, PRSS23, CCT5, GJA1, XPC, TAGLN2, SPTBN4, ARPC2, YWHAZ, CCT2, YWHAB, TUBA1A, CDK1, ACTG1, AKR1C3, TRABD2B
GO:0043209~myelin sheath	10	2.43E-07	2.26E-05	RALA, CDC42, WDR1, HSPA8, ACTR1A, ATP6V1B2, CCT5, CCT2, TUBA1A, ACTG1
GO:0005829~cytosol	35	2.56E-04	1.59E-02	TSPOAP1, TRAF1, CDC42, WDR1, TPX2, MYL12A, HSPA8, BAG2, RGS2, CENPF, HIF3A, WNK4, ACTR1A, TPM3, ALDH1L1, SH3KBP1, ATP6V1B2, CCT5, GJA1, OBSCN, SPTBN4, ARPC2, YWHAZ, WNK2, CCT2, YWHAB, SGSM1, TUBA1A, CDK1, PFKFB3, IL16, KPNA2, ACTG1, AKR1C3, ARHGAP11A
GO:0005925~focal adhesion	10	6.46E-04	3.00E-02	RALA, CDC42, HSPA8, CAP1, SH3KBP1, GJA1, ARPC2, YWHAZ, YWHAB, ACTG1

Supplementary Table 4 - Gene expression level differences upon upregulation of WWP2.

Category	Gene	Fold change	P-value
Cartilage markers	*COL2A1*	0.6	1.05E-02
	ACAN	0.8	3.45E-02
	SOX9	0.77	1.84E-01
	FN1	0.93	8.22E-01
Cartilage degeneration markers	*EPAS1*	1.56	4.19E-03
	POSTN	1.25	1.12E-01
	RUNX2	0.8	8.70E-02
	ADAMTS5	1.15	2.57E-01
Genes correlating to *WWP2*	*GDF10*	0.62	2.21E-03
	STC2	0.73	3.63E-02
	GJA1	0.76	8.28E-02
	WNK4	2.61	2.52E-01
	WDR1	0.98	5.36E-01

Supplementary Table 5 (partially) - Differential protein expression on day three and day seven relative to day zero of pellet culture in our 3D chondrocyte pellet cultures.
The top 50 proteins with highest abundance ratio da7/day0 are shown here, the rest of the table can be found in the online supplement: https://doi.org/10.1016/j.joca.2022.09.009

Accession	Name	# Peptides	# Unique Peptides	Abundance Ratio: day3/day0	Abundance Ratio: day7/day0
P27658	COL8A1	6	6	13.27	40.19
P02458	COL2A1	67	61	2.68	32.94
P22914	CRYGS	9	9	12.54	31.15
P02461	COL3A1	109	108	11.89	27.14
Q06828	FMOD	8	8	7.68	25.00
Q02388	COL7A1	7	7	6.74	23.52
P02452	COL1A1	109	105	7.03	22.97
P49747	COMP	21	21	5.31	20.25
Q07507	DPT	5	5	6.86	16.10
P08123	COL1A2	94	93	4.99	14.41
P16112	ACAN	43	43	5.28	13.75
Q15063	POSTN	39	39	4.31	12.43
O00339	MATN2	22	22	5.10	11.95
P12107	COL11A1	35	28	3.11	10.84
Q15782	CHI3L2	9	9	9.03	10.04
P51888	PRELP	12	12	4.07	9.67
P55001	MFAP2	4	4	5.28	9.44
P05090	APOD	7	7	5.83	9.43
P21810	BGN	12	11	3.73	9.34
Q8IUX7	AEBP1	38	37	3.90	8.02
P05997	COL5A2	50	48	3.61	7.87
P13611	VCAN	27	27	2.80	7.65
P20908	COL5A1	37	30	3.23	6.27
P07996	THBS1	34	33	3.19	6.06
P24821	TNC	106	106	3.45	5.86
P14555	PLA2G2A	4	4	1.90	5.79
Q07092	COL16A1	17	17	2.71	5.78
Q5JTB6	PLAC9	4	4	4.54	5.75
Q16790	CA9	6	6	4.47	5.54
Q8TF66	LRRC15	7	7	1.26	4.89
P10915	HAPLN1	15	15	2.86	4.39
P35555	FBN1	101	95	2.79	4.38

Accession	Name	# Peptides	# Unique Peptides	Abundance Ratio: day3/day0	Abundance Ratio: day7/day0
P02462	COL4A1	9	9	3.42	4.29
Q15582	TGFBI	33	33	3.30	4.17
Q6UX71	PLXDC2	7	7	2.61	4.16
P09486	SPARC	12	12	1.93	4.06
Q9Y6C2	EMILIN1	38	38	3.09	3.88
Q92954	PRG4	57	57	1.67	3.71
Q15113	PCOLCE	16	16	2.55	3.69
Q92743	HTRA1	10	10	2.69	3.53
P02751	FN1	98	98	2.12	3.51
P02795	MT2A	4	1	1.90	3.49
Q658P3	STEAP3	7	7	2.36	3.38
P35556	FBN2	17	11	3.00	3.34
Q14112	NID2	33	32	2.94	3.32
P02792	FTL	10	10	3.43	3.31
P12111	COL6A3	165	165	2.53	3.10
Q76M96	CCDC80	13	13	1.59	3.04
Q13451	FKBP5	21	20	2.77	3.02
Q14767	LTBP2	23	23	1.29	2.99

Supplementary Table 6 (partially) - Differential protein expression between chondrocyte pellet cultures with and without upregulation of WWP2.
The top 50 proteins with highest abundance ratio WWP2/control are shown here, the rest of the table can be found in the online supplement: https://doi.org/10.1016/j.joca.2022.09.009

Accession	Name	# Peptides	# Unique Peptides	Abundance Ratio: WWP2/control
O00308	WWP2	31	28	10.10
P09914	IFIT1	2	1	1.89
P26022	PTX3	2	2	1.78
Q16832	DDR2	2	2	1.53
Q96LR5	UBE2E2	4	2	1.52
P33897	ABCD1	2	2	1.52
P51965	UBE2E1	3	1	1.44
P28300	LOX	3	3	1.43
Q96B36	AKT1S1	2	2	1.38
Q9P2K8	EIF2AK4	3	3	1.37
Q969T4	UBE2E3	3	1	1.36
Q9UBX5	FBLN5	5	5	1.33
P54652	HSPA2	27	14	1.32
Q01780	EXOSC10	2	2	1.32
P21741	MDK	3	3	1.31
Q96GY0	ZC2HC1A	2	2	1.31
Q9Y4K4	MAP4K5	2	2	1.31
Q92541	RTF1	3	3	1.30
P05161	ISG15	3	3	1.30
P47974	ZFP36L2	2	1	1.30
P25205	MCM3	2	2	1.30
P61077	UBE2D3	3	2	1.30
P62837	UBE2D2	3	2	1.30
Q9Y4F5	CEP170B	2	2	1.30
Q13613	MTMR1	3	3	1.30
Q9H7D7	WDR26	2	2	1.29
O00148	DDX39A	14	3	1.29
Q5RI15	COX20	2	2	1.28
Q13586	STIM1	2	2	1.28
Q9Y625	GPC6	6	6	1.28
P55290	CDH13	6	6	1.27
Q9HA77	CARS2	4	4	1.26

Accession	Name	# Peptides	# Unique Peptides	Abundance Ratio: WWP2/control
Q9H6T3	RPAP3	2	2	1.26
Q9H2K8	TAOK3	3	2	1.26
Q5T9L3	WLS	2	2	1.26
Q5RKV6	EXOSC6	3	3	1.26
Q8IVF2	AHNAK2	15	13	1.26
Q8IWT0	ZBTB8OS	2	2	1.25
Q05655	PRKCD	3	2	1.25
O94804	STK10	7	6	1.25
Q96RK0	CIC	2	2	1.25
P83111	LACTB	4	4	1.25
Q9UM22	EPDR1	2	2	1.25
Q9BQE4	SELENOS	2	2	1.25
Q9HAV7	GRPEL1	2	2	1.25
P28845	HSD11B1	3	3	1.25
P29373	CRABP2	3	3	1.25
Q93062	RBPMS	2	2	1.24
Q5VWZ2	LYPLAL1	2	2	1.24
O43172	PRPF4	4	4	1.24

Supplementary Table 7 - Gene expression level differences upon upregulation of miR-140-3p.

Category	Gene	Fold change	P-value
WWP2 transcripts	*WWP2-FL*	1.22	1.63E-02
	WWP2-isoform2	0.92	3.29E-01
	WWP2-isoform4	0.63	1.63E-02
	WWP2-isoform6	1.29	5.67E-02
Genes correlating to *WWP2*	*WDR1*	1.79	1.19E-03
	STC2	1.55	7.51E-02
	GJA1	1.07	9.24E-01
	ACAN	0.88	2.44E-01